Spinodal decomposition as a probe to measure the effects on molecular motion in poly(styrene-co-acrylonitrile) and poly(methyl methacrylate) blends after mixing with a low molar mass liquid crystal or commercial lubricant

S. Wacharawichanant[a], S. Thongyai[a], S. Tanodekaew[b], J.S. Higgins[c,*], N. Clarke[d]

[a]*Department of Chemical Engineering, Chulalongkorn University, Phayathai Road, Bangkok 10330, Thailand*
[b]*National Metal and Materials Technology Center (MTEC), 114 Paholyothin Road, Klong 1, Klong Luang, Pathumthani 12120, Thailand*
[c]*Department of Chemical Engineering and Chemical Technology, Imperial College of Science, Technology and Medicine, Price Consort Road, London SW7 2BY, UK*
[d]*Department of Chemistry, University Science laboratories, University of Durham, South Road, Durham DH1 3LE, UK*

Abstract

The effects on molecular motion observed through early stage phase separation via spinodal decomposition, in melt mixed poly(styrene-co-acrylonitrile) (SAN) containing 25% by weight of acrylonitrile (AN) and poly(methyl methacrylate) (PMMA) (20/80 wt%) blends after adding two low molar mass liquid crystals (CBC33 and CBC53) and two lubricants (GMS and zinc stearate) were investigated using light scattering techniques. The samples were assessed in terms of the apparent diffusion coefficient (D_{app}) obtained from observation of phase separation in the blends. The early stages of phase separation as observed by light scattering were dominated by diffusion processes and approximately conformed to the Cahn–Hilliard linearised theory. The major effect of liquid crystal (LC) was to increase the molecular mobility of the blends. The LC generally increased the Cahn–Hilliard apparent diffusion coefficient, D_{app}, of the blend when added with concentrations as low as 0.2 wt%. GMS and zinc stearate can also improve the mobility of the blend but to a lesser extent and the effect does not increase at higher concentration. On the other hand, the more LC added, the higher the mobility. In all systems the second derivative of the Gibbs free energy becomes zero at the same temperature. The improved mobilities therefore seem to arise from changes in dynamics rather than thermodynamic effects.
© 2004 Elsevier Ltd. All rights reserved.

Keywords: Polymer blend; Phase separation; Spinodal decomposition

1. Introduction

It is well known that many properties of polymer blends are determined by their morphology and the relationships have been extensively investigated. Phase separation from an initially homogeneous mixture is considered to be one possible route to generate irregular spatial patterns in the samples. A partially miscible polymer blend generally undergoes spinodal decomposition after exposure to temperatures in the unstable two-phase regime. The rates of phase separation and the resulting morphology depend on many parameters, e.g. time of heat treatment, temperature, concentration, and physical properties of the blend constituents. Many publications have reported on the various stages of the growth of the spatial composition fluctuations and in this paper we concentrate on the early stages as described by linearised Cahn–Hilliard theory [1,2].

Many studies of the phase behaviour, miscibility and thermal properties in polymer and liquid crystal (LC) mixtures have been reported in recent years [3–11]. It has long been known that a LC can reduce the melt viscosity of polyolefins and polyester blends [14]. However, these effects are very similar to those induced by other small molecule addition especially lubricant additives such as zinc stearate. The lubricant molecules usually act as so-called

external lubricants, migrate to the surface of the melt polymer and metal, and this modifies the polymer viscosity at the metal interface. Consequently, it appears as if the viscosity of the blend has decreased. In an extensive series of experiments on blends with LCs [12,13] we have observed a reduction in the blend viscosity under shear, applied using both twin-plate and capillary rheometers. We have found that very small (less than 1%) amounts of LC can dramatically reduce the shear viscosity of the melt blend, but the mechanisms are still under investigation. At these low levels the glass transition temperatures are essentially unaltered. If the addition of LC contributes to the non-shear dynamics of the polymer molecules the mechanism of the reduction in melt viscosity would be different from that of the normal lubricants. This is an internal lubrication effect. The LC blends are usually transparent and this may imply miscibility at a molecular level. This is in contrast with normal lubricants, which are likely to phase separate at the molecular level.

In the course of investigating any effect of the added LCs on the phase behaviour of melt mixed SAN/PMMA (20/80) blends, it became clear that the kinetics of phase separation seemed to be speeded up, and we conjectured that this might be a sign that the added LCs were affecting the molecular segmental dynamics at a local level. This prompted a systematic investigation of the effect of LCs on the phase separation kinetics of these blends and a comparison with the effect of addition of normal lubricants. We report here light scattering data from samples undergoing phase separation via spinodal decomposition, and analyse the data in order to compare the mobility in the blends with and without additives.

2. Cahn–Hilliard theory

Within this model the equation of motion for concentration fluctuations is written as

$$\frac{\partial \delta\phi_q(t)}{\partial t} = -q^2 M \frac{\partial F[\delta\phi_q(t)]}{\partial \delta\phi_q(t)} \tag{1}$$

where M is a mobility and the Fourier transform of $\delta\phi(r,t)$ can be defined as,

$$\delta\phi_q(t) = \frac{1}{(2\pi)^{3/2}} \int dr \delta\phi(r,t)\exp\{-iqr\} \tag{2}$$

and $F[\delta\phi_q(t)]$ is the Fourier transformed Flory–Huggins–deGennes free energy, which can be written as,

$$F_{FH-dG}[\delta\phi_q(t)] = \sum_q \lfloor\chi_s - \chi + \kappa q^2\rfloor\delta\phi_q^2 \tag{3}$$

where χ_s is the value of the interaction parameter on the spinodal curve and κ is gradient energy. From Eqs. (2) and (3), the scattering function $S_q(t)$, defined as,

$$S_q(t) = \langle|\delta\phi_q(t)|^2\rangle \tag{4}$$

is found to be,

$$S_q(t) = S_0(0)\exp\{2R(q)t\} \tag{5}$$

where $R(q)$ is the q dependent growth rate of concentration fluctuations, given by,

$$R(q) = -q^2 M\left[\left(\frac{\partial^2 f}{\partial \phi^2}\right)_{\phi_0} + 2\kappa q^2\right] \tag{6}$$

The leading term on the right hand side of Eq. (6) leads to a definition of an apparent diffusion coefficient, D_{app}, which is the coefficient of the q^2 term. Because the second derivative of the free energy (f) becomes zero at the spinodal temperature T_s it can be seen that D_{app} also becomes zero at T_s. Generally, the growth or decay with time depends on whether $R(q)$ is positive or negative. In the metastable region, $R(q)$ is always negative; consequently concentration fluctuation always decay. On the other hand, in the unstable region where the blend undergoes spinodal decomposition, $R(q)$ is positive for q less than the critical value (q_c), indicating that the fluctuation grows with time. The critical value q_c can be expressed as,

$$q_c = \sqrt{-\frac{(\partial^2 f/\partial \phi^2)_{\phi_0}}{2\kappa}} \tag{7}$$

Eq. (7) has a maximum at

$$q_m = \frac{1}{2}\sqrt{-\frac{(\partial^2 f/\partial \phi^2)_{\phi_0}}{2\kappa}} \tag{8}$$

Inserting the maximum wave vector q_m into Eq. (6), the highest relative growth rate $R(q_m)$ is:

$$R(q_m) = \frac{M}{8\kappa}\left(\frac{\partial^2 f}{\partial \phi^2}\right)_{\phi_0}^2 \tag{9}$$

Apparent diffusion coefficients, D_{app} are defined as,

$$D_{app} = -M\left(\frac{\partial^2 f}{\partial \phi^2}\right)_{\phi_0} \tag{10}$$

or alternatively

$$D_{app} = \frac{2R(q_m)}{q_m^2} \tag{11}$$

From Eq. (6), a plot of $R(q)/q^2$ vs. q^2 should yield a straight line with a slope of $2MK$ and an intercept of D_{app}. Furthermore, q_m and $R(q_m)$ also can be obtained from these slopes and intercepts as follows,

$$q_m = \sqrt{\frac{Intercept}{-2Slope}} \tag{12}$$

$$R(q_m) = \frac{(Intercept)^2}{-4Slope} \tag{13}$$

The mobility term M in the equations above deserves some discussion. It is a combination of the dynamic

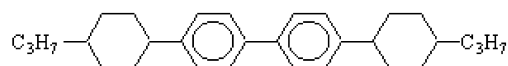Fig. 1. Structure of CBC33.

Table 1
Properties of low molar mass thermotropic liquid crystals

Property	CBC33	CBC53
Melting point (°C)	158	164
Smectic-nematic temperature (°C)	223	260
Clearing temperature (°C)	327	317
Molecular weight (g/mol)	403	431

properties of the components of the blend and the exact way that combination is formed has been the subject of considerable discussion in the literature. (See for example Meier et al. [19] and more recently, Kamath et al. [20].)

In case of an intimate mixture of the LC with the blend, M may be expected to be sensitive to the LC addition. Other ways of observing this effect would include direct measurement of the viscosity—though we have already remarked on the confusing effect of surface segregation—and various spectroscopies observing the local dynamics directly. However, as we were particularly interested in the miscibility behaviour, it seemed worthwhile to investigate how much information of the mobility effect of the LCs was available from this route.

3. Experimental section

3.1. Materials and sample preparation

The random copolymer of poly(styrene-co-acrylonitrile) (SAN) containing about 25% by weight of acrylonitrile (AN) was kindly provided by Bayer Polymers Co., Ltd. It appears as slightly yellowish transparent pellets with a glass transition temperatures (T_g) at 105 °C. The commercial grade polymethyl methacrylate (PMMA) was kindly provided by TPI polyacrylate Co., Ltd. and for this samples Tg is 95 °C. Both materials were kept in a dry atmosphere and heated prior to use. SAN and PMMA were heated at 130 °C in a vacuum oven for 4 h in order to remove any water.

Low molar mass thermotropic liquid crystals were purchased from Merck Co., Ltd. CBC33 and CBC53 are in the form of a white powder. Their structures which contain a cyclohexyl-biphenyl-cyclohexane backbone are shown as Figs. 1 and 2, respectively. Molecular weight characteristics, transition temperatures, and other physical properties are shown in Table 1.

The lubricant, glycerol monostearate (GMS) was kindly provided by Rikevita Ltd (Malaysia). The melting point is 65 °C and the molecular weight is 358 g/mol zinc stearate with molecular weight 632 g/mol, was supplied by Quality Minerals Co., Ltd. The chemical structure of GMS and zinc stearate are shown in Figs. 3 and 4, respectively.

Melt mixed blends of 20/80 (weight ratio) SAN/PMMA were obtained using a PRISM twin screw extruder, which was operated at a torque of 60%, the screw speed of 30 rpm
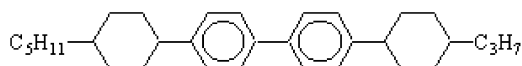
and the processing temperature range was 190–210 °C. The extrudate was cut into small beads using a PRISM pelletiser and the transparent beads were compression moulded using a hot press at 180 °C, which is still inside the miscible regime for this blend (see Fig. 8). Thin films (approximately 0.05–0.10 mm) were used for light scattering experiments.

The blends of pre-mixed SAN/PMMA and LC or lubricant were prepared by using a digital hot plate at the compositions of 0.2, 0.4 and 1% by weight of LC and lubricant. We mixed the pre-mixed SAN/PMMA and LC or lubricant together at 200 °C for 20 min, then compression moulded at 180 °C. Note that both temperatures are still inside the miscible regime for this blend.

3.2. Equipment and methods

3.2.1. Small angle light scattering (SALS)

The study of miscibility was performed using light scattering apparatus at the Department of Chemical Engineering, Chulalongkorn University, Thailand.

A He/Ne laser of 5 mW ($\lambda = 632.8$ nm) is used as an incident light source. Samples were placed on a LINKAM hot stage, which was mounted between the laser and a CCD camera. The temperature of the LINKAM hot stage was controlled by a computer. The light scattering pattern is captured by a CCD camera. The light scattering pattern was analysed using the Image-Pro Plus 3.0 program.

The experiment was designed to determine the D_{app} and the spinodal temperature by following the spinodal decomposition process after a temperature jump from the one phase to the two phase region. The difference between the phase separation temperature and T_s is called the quench depth. Homogeneous blends were annealed at a temperature which is about 20 °C below the desired phase separation temperature and below the cloud point for at least 15 min and then transferred quickly into the LINKAM hot stage, which was preheated to the desired temperature inside the phase boundary. The rate of change of intensity with time (after any delay time) of scattered light patterns provides the Cahn–Hilliard growth rate ($R(q)$) [1,2] from Eq. (5) as seen in Fig. 5, D_{app} can then be obtained as in Eq. (6) from the intercept of a plot of $R(q)/q^2$ vs. q^2 as shown in Fig. 6.
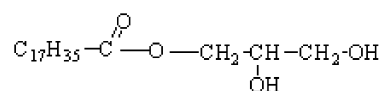

Fig. 2. Structure of CBC53.

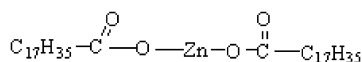Fig. 3. Structure of glycerol monostearate (GMS).

Fig. 4. Structure of zinc stearate.

However, it should be noted that the data in Fig. 6 are not linear. The effects have been attributed to thermal fluctuations or to polymer relaxation [15] but are more likely to arise because we are not observing the really early stages of spinodal decomposition—as witnessed by the apparent time delay before growth in Fig. 5. According to Cahn–Hilliard theory, the phase separation via spinodal decomposition should occur spontaneously after heating into the phase separation regime. It was however found that a delay time frequently appeared at the beginning of phase separation (shown in Fig. 5). The response time of the light scattering used in this work is not causing a problem. Refs. [16,17] show that for at least some blends there is growth in a wavelength range not observable by light scattering, and this may well be the case here. While this means that the really early stages will be missed, and will lead to the data not following Cahn–Hilliard theory—as discussed later on—we will argue that the conclusions about changes in the growth rates $R(q)$ observed when adding small molecules are still valid.

We chose to extrapolate the high q-data range to obtain the values of D_{app}, as this is less likely to be contaminated by any initial inhomogeneities in the sample often supposed to be dust or unmixed polymers. Spinodal temperatures, T_s (or apparent values of T_s) can be obtained by extrapolating the apparent diffusion coefficient to zero as shown in the insert in Fig. 6. The values of T_s obtained in this way are included with the cloud point data in Fig. 8. The discrepancies between T_s and T_c probably arises because of this difficulty in obtaining the true early stages from light scattering. However, it should be noted that phase separation becomes possible once the binodal curve has been crossed so that for off critical blends in a continuous heating experiment, the cloud point may detect the binodal or occur at some point apparently between the binodal and spinodal.

4. Results and discussion

4.1. Phase behaviour

The point at which the scattered intensities start to increase in data such as that shown in Fig. 7 is defined as the cloud point (T_c). Apparent cloud point values depend on the rate at which phase separation in the sample responds to the temperature changes, and, the lower the heating rate the lower the cloud point value. Extrapolating heating rate to zero is then used to obtain a value close to the true cloud point. For our cloud point measurement several heating rates (0.3, 0.5, 1.0 °C/min) were chosen. Extrapolating to zero heating rate as shown in the insert in Fig. 7 was used to obtained the cloud point.

Cloud point curves for SAN/PMMA blends are shown in Fig. 8. The blends, which are first clear, become cloudy after heating, indicating lower critical solution temperature (LCST) behaviour. Fig. 8 shows the cloud point temperatures for blends containing SAN copolymers with varying AN content, all extrapolated to zero heating rate. It has previously been noted that the phase behaviour depends on the amount of AN in SAN copolymer [18]. The SAN copolymer used in this study contained about 25 wt% of AN. The lower the AN content in the copolymer, the lower the SAN wt% at the critical point of the blends. The data for the cloud points and the spinodal of the 25% AN blend in Fig. 8, suggest that the critical composition should be between 10 and 20 wt% of SAN. The separation temperatures
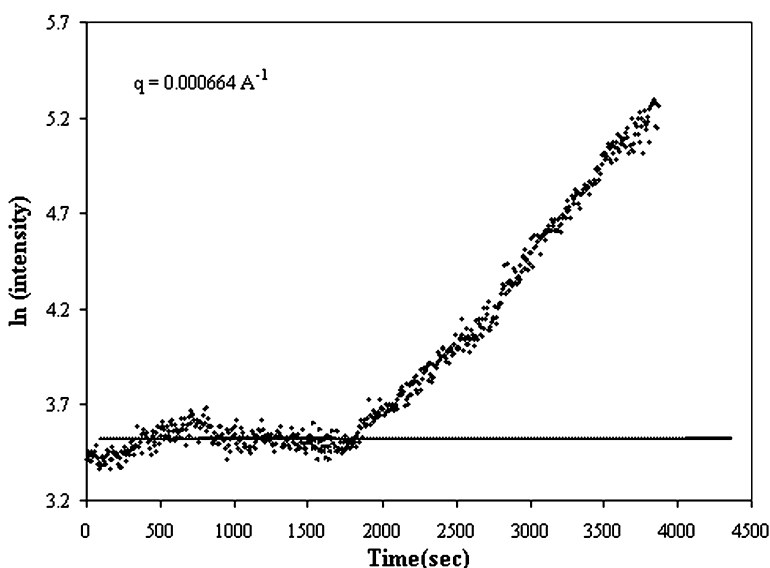

Fig. 5. A plot of ln(Intensity) against time for SAN/PMMA (20/80) blends, obtained from a temperature jump experiment at 217 °C. As seen in this figure, the delay time is approximately 1700 s.
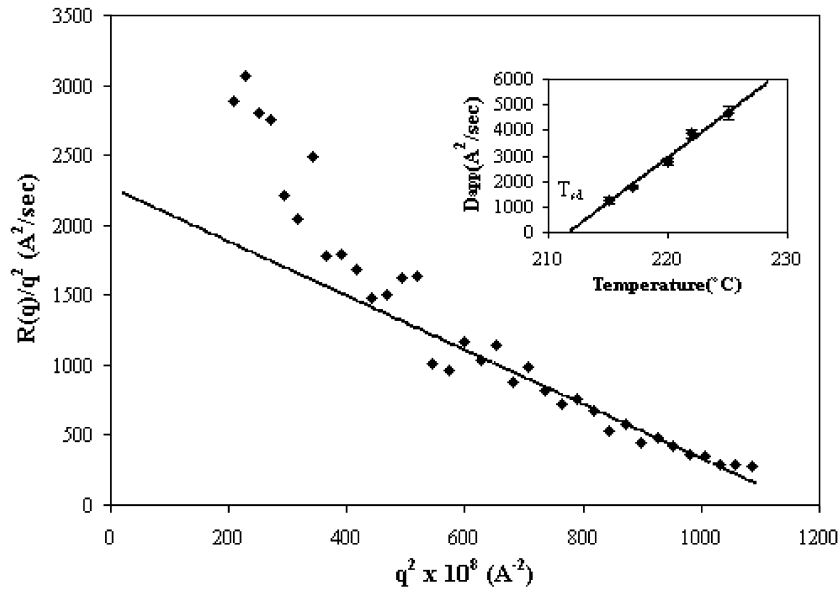
Fig. 6. A plot of $R(q)/q^2$ against q^2 for SAN/PMMA (20/80) blends after adding 0.2 wt% CBC53, obtained from a temperature jump at 220 °C. The range of q^2 between 2×10^{-10} and 12×10^{-10} Å^{-2} was chosen to find D_{app}. Insert: the spinodal temperature (T_{sd}) can be obtained from extrapolating D_{app} to zero.

are falling as we reduce the amount of SAN in the blend, but while we can detect a cloud point at 20%, we cannot find any phase separation as we raise the temperature for concentration of 10%. Moreover, from Ref. [18], SAN/PMMA blends usually have a critical point below 20 wt% SAN as shown by some literature values in Fig. 8. For these reasons we chose this composition to study the effects of molecular movement of polymer after adding LCs and normal lubricants.

4.2. Growth rate ($R(q)$)

As already remarked these samples show an apparent induction period after a temperature jump inside the

spinodal as seen in Fig. 5. We estimated growth rates $R(q)$ from the slopes of ln(intensity) vs. t plots after this induction period—in order to compare the kinetics of the phase separation for the different samples. Strictly these should be called apparent values of $R(q)$ until it is possible to obtain information about what is happening at larger q-values during this induction period. However, we believe even with these caveats that the data provide a reasonable method of comparing rates in different samples, though absolute values should be treated with discretion. The growth rates, $R(q)$, are shown in Fig. 9 as a function of q for pure blends and the blends with CBC53 and GMS, respectively, all at 220 °C. $R(q)$ values obtained from the phase separated blends with added LCs are clearly higher than for the original blend. We
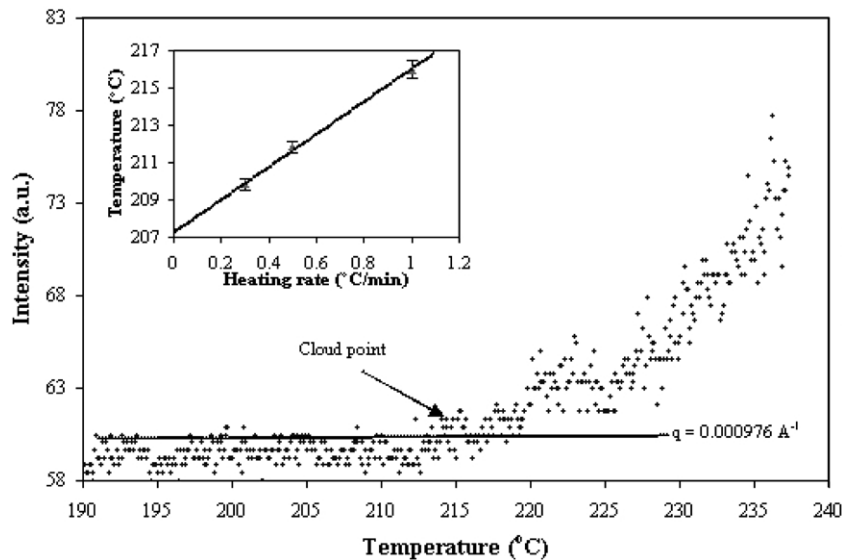

Fig. 7. A plot of intensity against temperature for SAN/PMMA (40/60) blend at the heating rate of 1.0 °C/min. Insert: the heating rate dependence of cloud point temperatures.
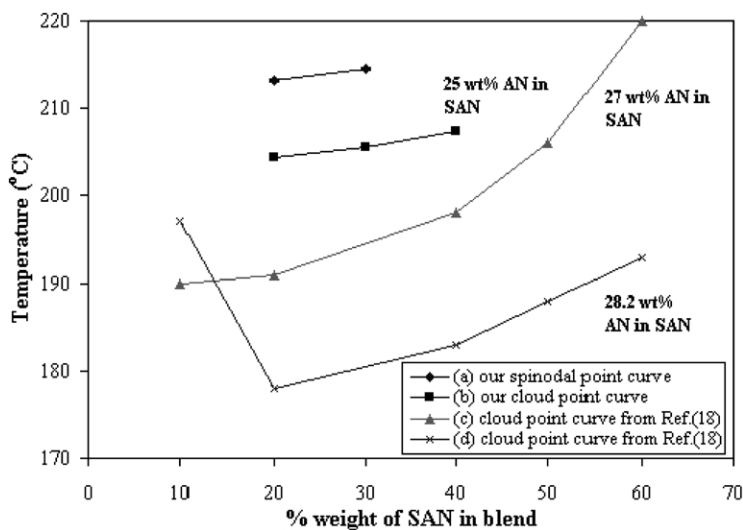
Fig. 8. Phase diagram of SAN/PMMA determined by light scattering technique. The cloud points were obtained by extrapolation to zero heating rate (a)–(b) $\bar{M}_w$ of PMMA is 72,575, $\bar{M}_w$ of SAN is 149,926, (c) $\bar{M}_w$ of PMMA is 167,000, $\bar{M}_w$ of SAN is 82,000, (d) $\bar{M}_w$ of PMMA is 178,000, $\bar{M}_w$ of SAN is 83,000.

Table 2
The q_m values and phase separation temperatures for SAN/PMMA (20/80) blends before and after adding 1.0 wt%

Temperature (°C)	q_m (Å^{-1})					
	2:8 SAN/PMMA		2:8 SAN/PMMA + 1.0% CBC33		2:8 SAN/PMMA + 1.0% GMS	
	Observation	Calculation	Observation	Calculation	Observation	Calculation
215	0.000670	0.000825	0.000687	0.000826	0.000713	0.000823
217	0.000650	0.000818	0.000687	0.000814	0.000670	0.000819
220	0.000640	0.000774	0.000697	0.000832	0.000683	0.000822
222	0.000640	0.000824	0.000720	0.000835	0.000690	0.000824
225	0.000653	0.000817	0.000693	0.000830	0.000697	0.000838

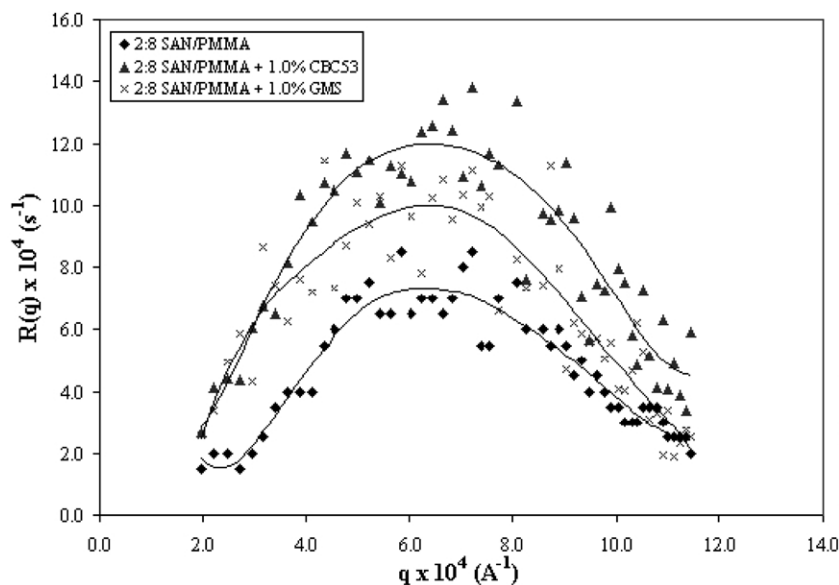CBC33 and GMS, obtained from direct observation and calculation methods.

Fig. 9. Plots of $R(q)$ against q for SAN/PMMA (20/80) blends before and after adding 1.0 wt% CBC53 and GMS, obtained from a temperature jump at 220 °C. (The lines are guides to the eye.)
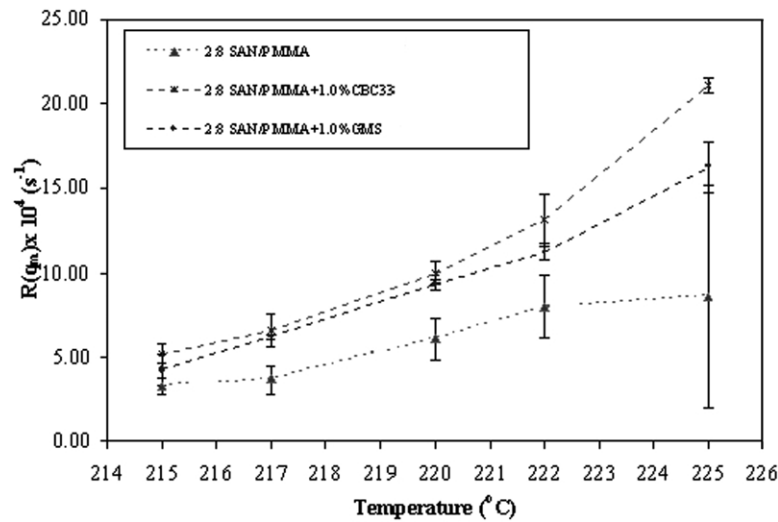
Fig. 10. The $R(q_m)$ values and phase separation temperatures for SAN/PMMA (20/80) blends before and after adding 1.0 wt%. CBC33 and GMS, obtained from direct observation method.

suggested that this might be the result of the increased molecular mobility after adding LCs and lubricants.

4.3. The maximum scattering wave number (q_m)

The maximum wave number, q_m, can be obtained from direct observation of data such as that in Fig. 9, and also calculated from the data plotted according to the Cahn–Hilliard theory as in Fig. 6 using Eq. (12). It can be seen in Table 2, where data from these two methods are compared, that the calculated values are slightly higher than those from direct observation, but both sets are essentially independent of temperature. The 5–10% discrepancy in values of q_m arise as a consequence of the failure of the Cahn–Hilliard theory to describe the data in Fig. 6. The experimental values of $R(q)$ do not vary parabolically with q^2 as demanded by the theory. As discussed earlier this is probably due to the fact that light scattering cannot detect the true early stages of spinodal decomposition where the domain sizes may be much smaller than the wavelength of light. Despite this failure we believe a comparison of behaviour between samples will be possible and note that values of q_m vary only very slightly with addition of LCs or lubricants but this is within experimental error.

4.4. The maximum growth rate ($R(q_m)$)

Fig. 10 shows the values of the maximum growth rate, $R(q_m)$, obtained by direct observation as a function of temperature for the blends before and after adding LCs. It can be seen that $R(q_m)$ increases fairly linearly with temperature in this region. This is to be expected both, because of the increased molecular mobility at higher temperatures, and the increased thermodynamic driving force at deeper quench depths. What is noticeable also is that the values of $R(q_m)$ for the pure blend are lower than the values of $R(q_m)$) of blends after adding LCs.

4.5. The apparent diffusion coefficient (D_{app})

Three criteria delimit the early stage spinodal decomposition, namely an exponential growth in the intensity of scattered light, time independence of q_m and the consistency of the data with Cahn–Hilliard theory through Eq. (6). As remarked above we believe that the discrepancies with C–H theory in Fig. 6 and the occurrence of a sizeable delay time indicate we may be missing the true early stages because the domain sizes are too small to be detected. Nevertheless, we believe that D_{app} values obtained by applying Eqs. (1)–(13) to analyse the data allow us to make a qualitative

Table 3

D_{app} and phase separation temperatures for SAN/PMMA (20/80) blends after adding CBC53 at various compositions

Sample	D_{app} at various temperature (Å^2/s)				
	215	217	220	222	225
2:8 SAN/PMMA	880.29	950.30	1581.12	2154.96	3884.87
2:8 SAN/PMMA + 0.2% CBC53	1476.74	1797.44	2765.34	3870.71	4686.70
2:8 SAN/PMMA + 0.4% CBC53	1574.50	2036.16	3028.86	4200.93	5771.12
2:8 SAN/PMMA + 1.0% CBC53	1335.31	2361.16	3305.13	4445.17	6379.92

comparison of results from different samples, even if the numerical values are themselves not meaningful.

Eq. (10) shows that D_{app} becomes zero at the spinodal temperature. Interestingly, even if we have estimated D_{app} from $R(q)$ data after the earliest stages we have generally found that the values extrapolate to zero at or close to the true spinodal. Hence although in this case we have obtained D_{app} from data after the apparent induction period and therefore probably not falling in the early stages—as described above, we believe the values of the spinodal temperatures will not be far from the true values. They are all in the range of $211.5 \pm 1.0\,°C$ for blends with and without additives.

The spinodal decomposition temperatures obtained in this way thus did not vary outside the experimental accuracy, indicating that the thermodynamics in the blends were not significantly altered by the addition of the small percentage of lubricants or LCs.

Table 3 lists the values of the D_{app} of SAN/PMMA (20/80) blends at various phase separation temperatures after adding CBC53 in varying amounts compositions. These

data show that as suggested by the $R(q)$ values in Fig. 10, the D_{app} values increase both with LC composition and with phase separation temperatures (the latter, as expected from Cahn–Hilliard theory).

The D_{app} for samples containing CBC53 are significantly higher than those for the pure blends, particularly at larger quench depths. If we assume that the thermodynamic term in Eq. (10) is essentially unaffected by adding LCs (as witnessed by the fact that the cloud point temperatures do not shift), then D_{app} is determined by the molecular mobility term M. The implication is that small additions of LC significantly increase M. In Tables 4–6, we see that CBC33, GMS and zinc stearate all cause, the D_{app} values to increase with composition and temperature in the same way as CBC53.

However, for deeper quenches, the LC addition appears to significantly increase molecular mobility while the effect of the lubricants is very small. As argued above, since the spinodal temperature, and therefore the thermodynamic term in D_{app} are unaltered by addition of small molecules, we are led to the conclusion that the mobility term M is

Table 4

D_{app} and phase separation temperatures for SAN/PMMA (20/80) blends after adding 0.2 wt% of zinc stearate, GMS, CBC33 and CBC53

Sample	D_{app} at various temperature (Å²/s)				
	215	217	220	222	225
2:8 SAN/PMMA	880.29	950.30	1581.12	2154.96	3884.87
2:8 SAN/PMMA + 0.2% zinc stearate	1097.77	1617.02	1988.95	3147.92	3912.67
2:8 SAN/PMMA + 0.2% GMS	1169.40	1572.85	2273.05	2990.94	3942.20
2:8 SAN/PMMA + 0.2% CBC33	1472.11	1751.10	2339.12	3724.13	4428.73
2:8 SAN/PMMA + 0.2% CBC53	1476.74	1797.44	2765.34	3870.71	4686.70

Table 5

D_{app} and phase separation temperatures for SAN/PMMA (20/80) blends after adding 0.4 wt% of zinc stearate, GMS, CBC33 and CBC53

Sample	D_{app} at various temperature (Å²/s)				
	215	217	220	222	225
2:8 SAN/PMMA	880.29	950.30	1581.12	2154.96	3884.87
2:8 SAN/PMMA + 0.4% zinc stearate	1225.66	1417.85	2122.78	3110.51	4132.94
2:8 SAN/PMMA + 0.4% GMS	1403.41	1667.69	2573.37	2823.81	4191.22
2:8 SAN/PMMA + 0.4% CBC33	1806.54	2129.89	3115.63	3812.59	5540.89
2:8 SAN/PMMA + 0.4% CBC53	1574.50	2036.16	3028.86	4200.93	5771.12

Table 6

D_{app} and phase separation temperatures for SAN/PMMA (20/80) blends after adding 1.0 wt% of zinc stearate, GMS, CBC33 and CBC53

Sample	D_{app} at various temperature (Å²/s)				
	215	217	220	222	225
2:8 SAN/PMMA	880.29	950.30	1581.12	2154.96	3884.87
2:8 SAN/PMMA + 1.0% zinc stearate	1010.80	1638.78	2414.68	3424.97	4300.78
2:8 SAN/PMMA + 1.0% GMS	1180.49	1504.55	2519.40	2969.87	4094.78
2:8 SAN/PMMA + 1.0% CBC33	1530.79	2313.36	3024.74	4009.64	5736.16
2:8 SAN/PMMA + 1.0% CBC53	1335.31	2361.16	3305.13	4445.17	6379.92

being significantly increased, in effect that the LC additives are aiding molecular motion.

5. Conclusions

The rate at which structures develop in the early (or fairly early) stages of spinodal decomposition observed using light scattering allow us to obtain a measure of the mobility of the molecules during the phase separation and the effect on this of variable amounts of additives within the blend. We can obtain indicative values of D_{app} for the polymer blend systems in the spinodal region and use it to estimate the lubrication activity of the small molecular additives at the same temperatures. There are possibly very small effects of the lubricants on the molecular mobility during phase separation, but quite clear effects of addition of LC molecules can be observed, particularly for the deeper quenches. Thus the mechanism, which reduces the melt viscosity in blends may not be the same for LC and normal lubricants. Further experiments at a molecular level, for example NMR, may unveil the mechanism of the melt viscosity reduction in the LC blends.

Acknowledgements

References

[1] Hashimoto T. In: Cahn RW, Haasen P, Kramer EJ, editors. Structure of polymer blends. Materials science and technology, vol. 12. Chichester: Wiley; 1991. p. 251–300.
[2] Jinnai H, Hasegawa H, Hashimoto T, Han CC. J Chem Phys 1993;99: 4845–54.
[3] Ballauff M. Mol Cryst Liquid Cryst 1986;136:175–95.
[4] Ahn W, Kim CY, Kim H, Kim SC. Macromolecules 1992;25:5002–7.
[5] Kim JY, Cho CH, Palffy-Muhoray P, Mustafa M, Kyu T. Phys Rev Lett 1993;71:2232–9.
[6] Zhang H, Li F, Yang Y. Sci Chin, Ser B 1995;38:412–21.
[7] Shen C, Kyu T. J Chem Phys 1995;102:556–62.
[8] Chiu HW, Kyu T. J Chem Phys 1995;103:7471–81.
[9] Kyu T, Shen C, Chiu HW. Mol Cryst Liquid Cryst 1996;287: 27–34.
[10] Chiu HW, Zhou ZL, Kyu T. Macromolecules 1996;29:1051–8.
[11] Rodrigues JRS, Kaito A, Soldi V, Pires ATN. Polym Int 1998;46: 138–42.
[12] Chuenchaokit A. Master Degree Thesis. Bangkok: Chulalongkorn University; 1998.
[13] Powanusorn S. Master Degree Thesis. Bangkok: Chulalongkorn University; 2000.
[14] Buckley A, Conciatori AB, Calundann GW. US Patent 4,434,262; 1984.
[15] Rojanapitayakorn P, Thongyai S, Higgins JS, Clarke N. Macromolecules 2001;42:3475–87.
[16] Cabral JT, Higgins JS, Yeruna NA, Magonov SN. Macromolecules 2002;35:1941–50.
[17] Cabral JT, Higgins JS, McLeish TCB, Strausser S, Magonov SN. Macromolecules 2000;34:3748–56.
[18] Suess M, Kressler J, Kammer HW. Polymer 1987;28:957–60.
[19] Meier G, Fytas G, Momper B, Fleischer G. Macromolecules 1993;26: 5310–5.
[20] Kamath S, Colby RH, Kamur SK. Macromolecules 2003;36: 8567–73.